Supplement of E&G Quaternary Sci. J., 74, 169–192, 2025
https://doi.org/10.5194/egqsj-74-169-2025-supplement

Open Access E&G Quaternary Science Journal

Supplement of

Luminescence dating of alluvial sediments from the Quaternary fan–terrace sequence of the lower Bruche valley, Upper Rhine Graben, France

Madhurima Marik et al.

Correspondence to: Madhurima Marik (madhurima.marik@geologie.uni-freiburg.de)

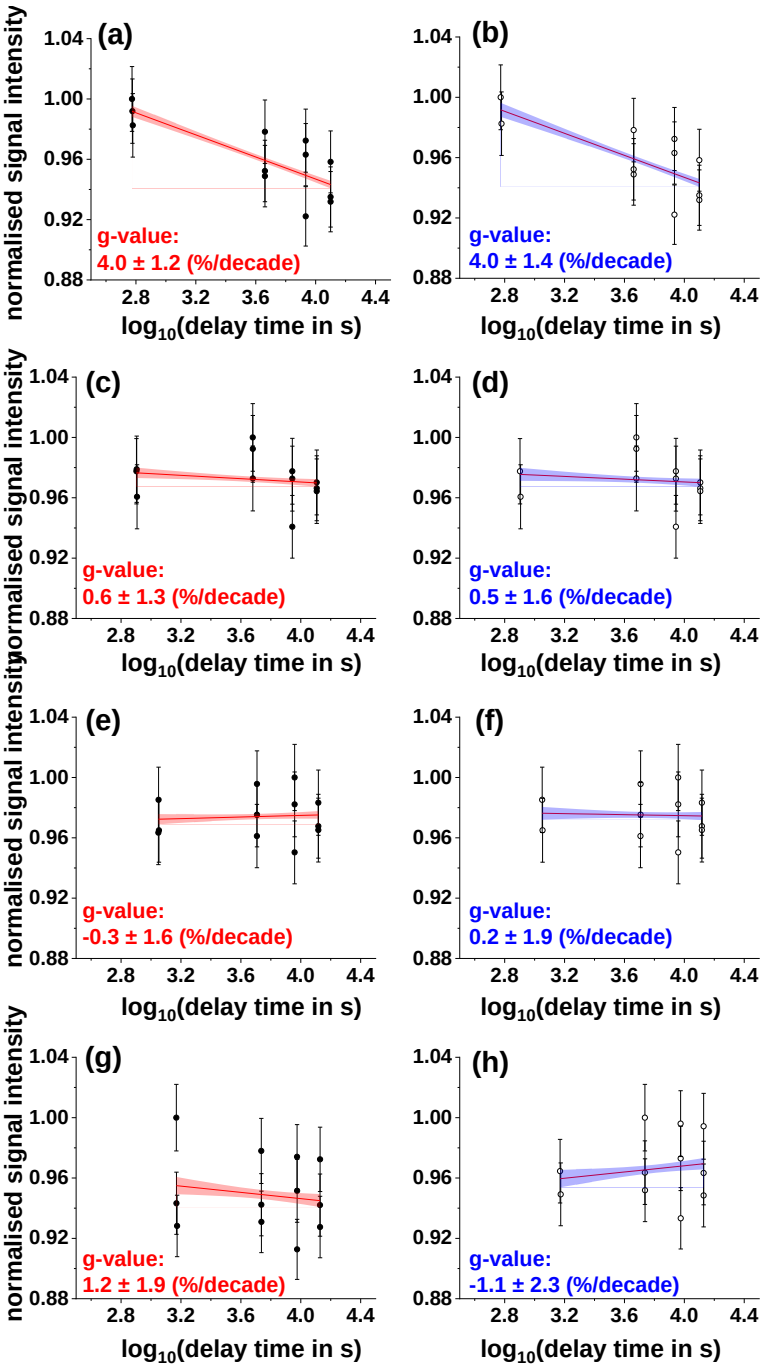

Figure S1. Anomalous fading measurements obtained for different IR stimulation temperatures with and without including the first prompt measurement, for a representative aliquot from sample RTSM. Normalized signal intensities are plotted as a function of time since irradiation for IR_{50} (a, b), pIR_{110} (c, d), pIR_{170} (e, f), and pIR_{225} (g, h) stimulations. Panels a, c, e, and g show the linear regression and corresponding fading rates (g-values norm. 2 days) measured for different delay times, while panels b, d, f and h excluding the first prompt. Fading rates were calculated using the *analyse_FadingMeasurement* function in R package luminescence version 0.9.23 (Kreutzer et al., 2012).

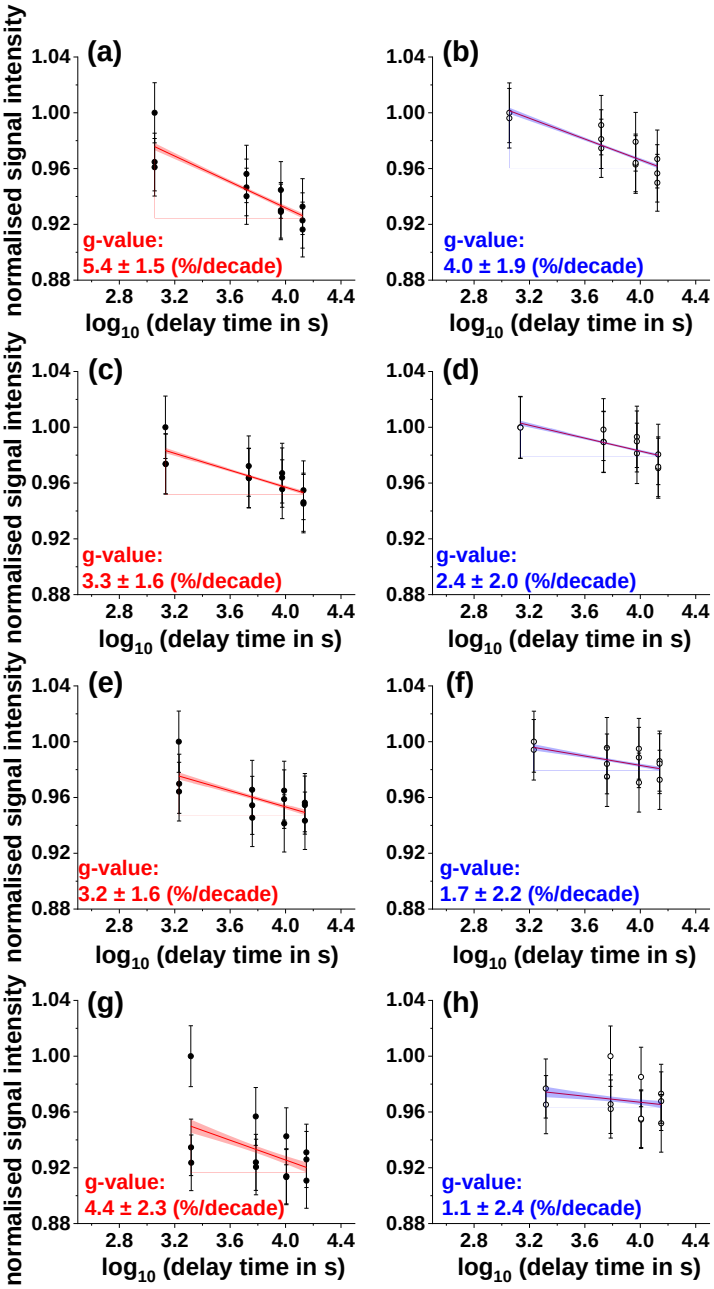

Figure S2. Anomalous fading measurements obtained for different IR stimulation temperatures with or without including the first prompt measurement, for a representative aliquot from sample LSSL1. Normalized signal intensities are plotted as a function of time since irradiation for IR_{50} (a, b), pIR_{110} (c, d), pIR_{170} (e, f), and pIR_{225} (g, h) stimulations. Panels a, c, e and g show the linear regression and corresponding fading rates (g-values norm. 2 days) obtained including all signal readouts measured at different delay times, while panels b, d, f and h excluding the first prompt. Fading rates were calculated using the *analyse_FadingMeasurement* function in R package luminescence version 0.9.23 (Kreutzer et al., 2012).

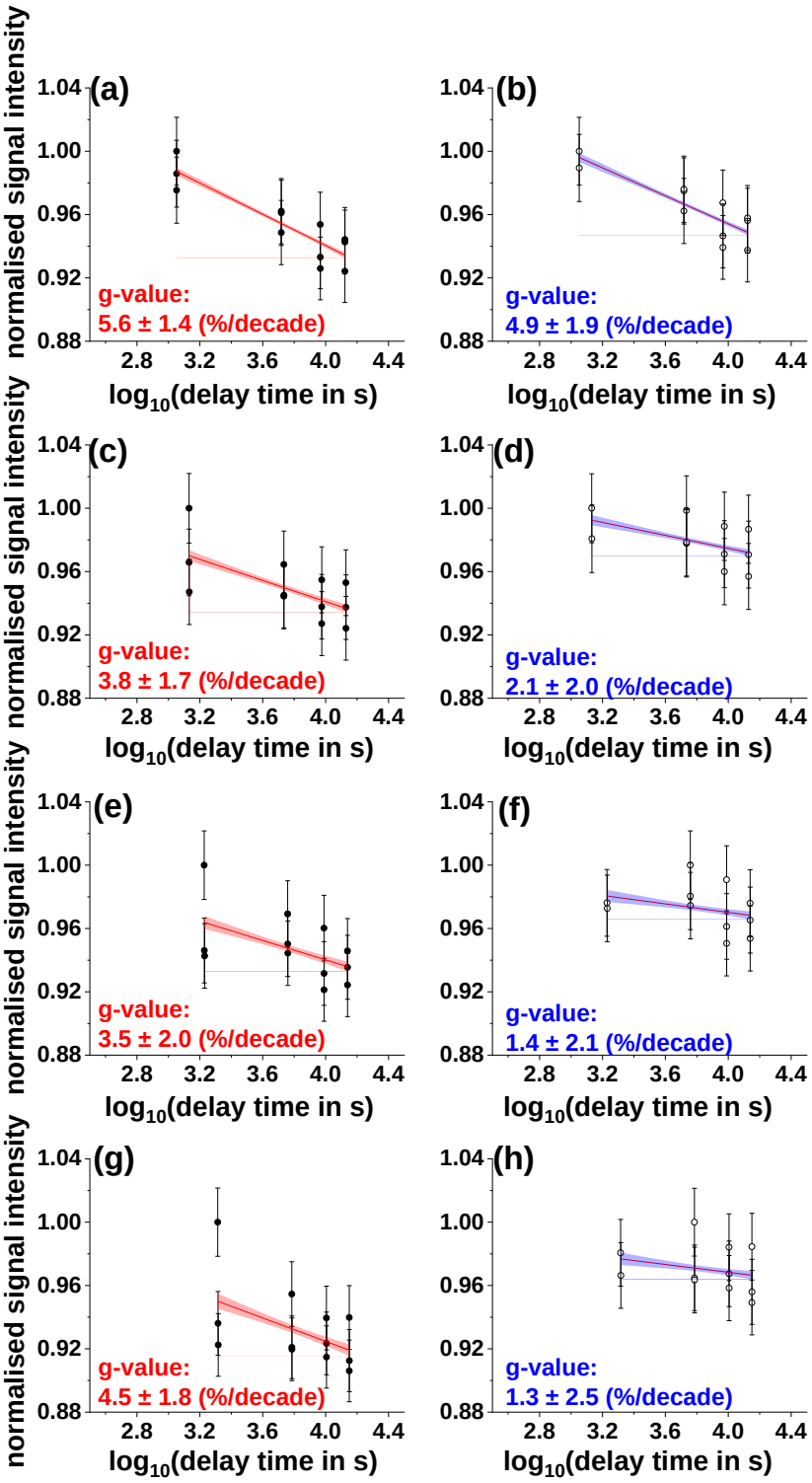

Figure S3. Anomalous fading measurements obtained for different IR stimulation temperatures with or without including the first prompt measurement, for a representative aliquot from sample LSSM. Normalized signal intensities are plotted as a function of time since irradiation for IR_{50} (a, b), pIR_{110} (c, d), pIR_{170} (e, f), and pIR_{225} (g, h) stimulations. Panels a, c, e and g show the linear regression and corresponding fading rates (g-values norm. 2 days) obtained including all signal readouts measured at different delay times, while panels b, d, f and h excluding the first prompt. Fading rates were calculated using the *analyse_FadingMeasurement* function in R package 'Luminescence' version 0.9.23 (Kreutzer et al., 2012).

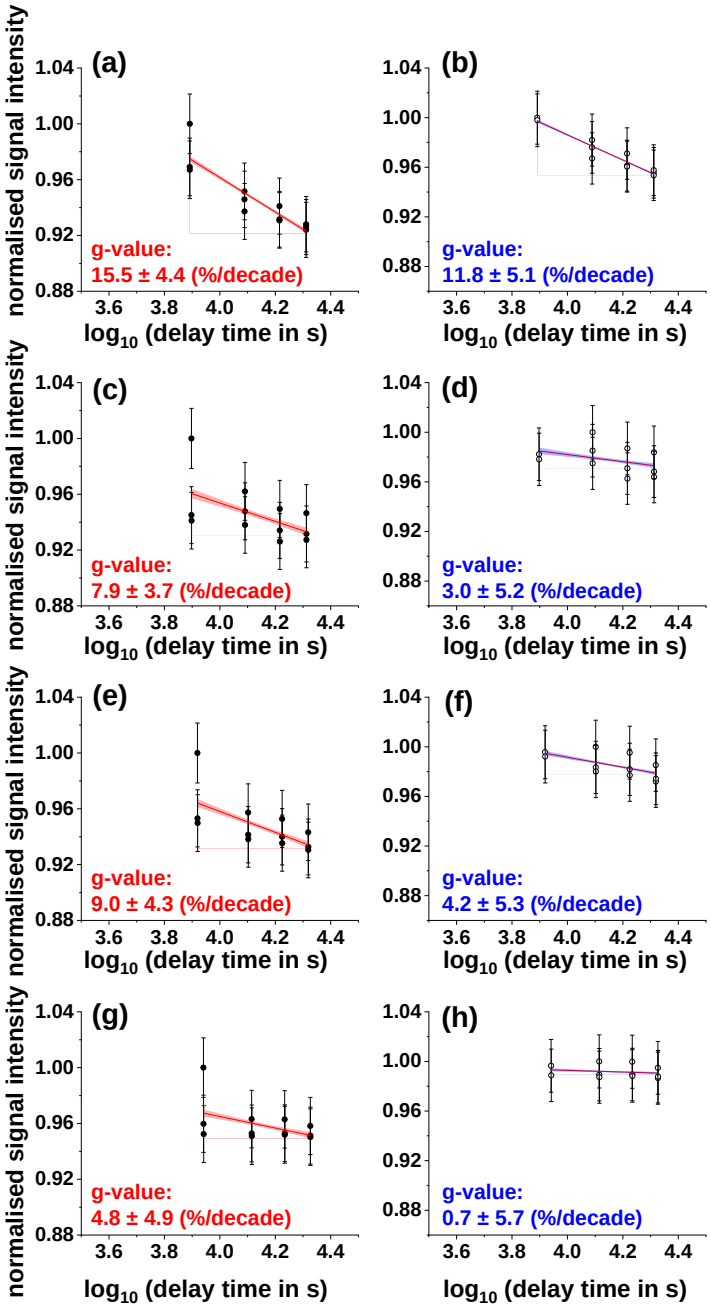

Figure S4. Anomalous fading measurements obtained for different IR stimulation temperatures with or without including the first prompt measurement, for a representative aliquot from sample GSSL1. Normalized signal intensities are plotted as a function of time since irradiation for IR_{50} (a, b), pIR_{110} (c, d), pIR_{170} (e, f), and pIR_{225} (g, h) stimulations. Panels a, c, e and g show the linear regression and corresponding fading rates (g-values norm. 2 days) obtained including all signal readouts measured at different delay times, while panels b, d, f and h excluding the first prompt. Fading rates were calculated using the *analyse_FadingMeasurement* function in R package 'Luminescence' version 0.9.23 (Kreutzer et al., 2012).

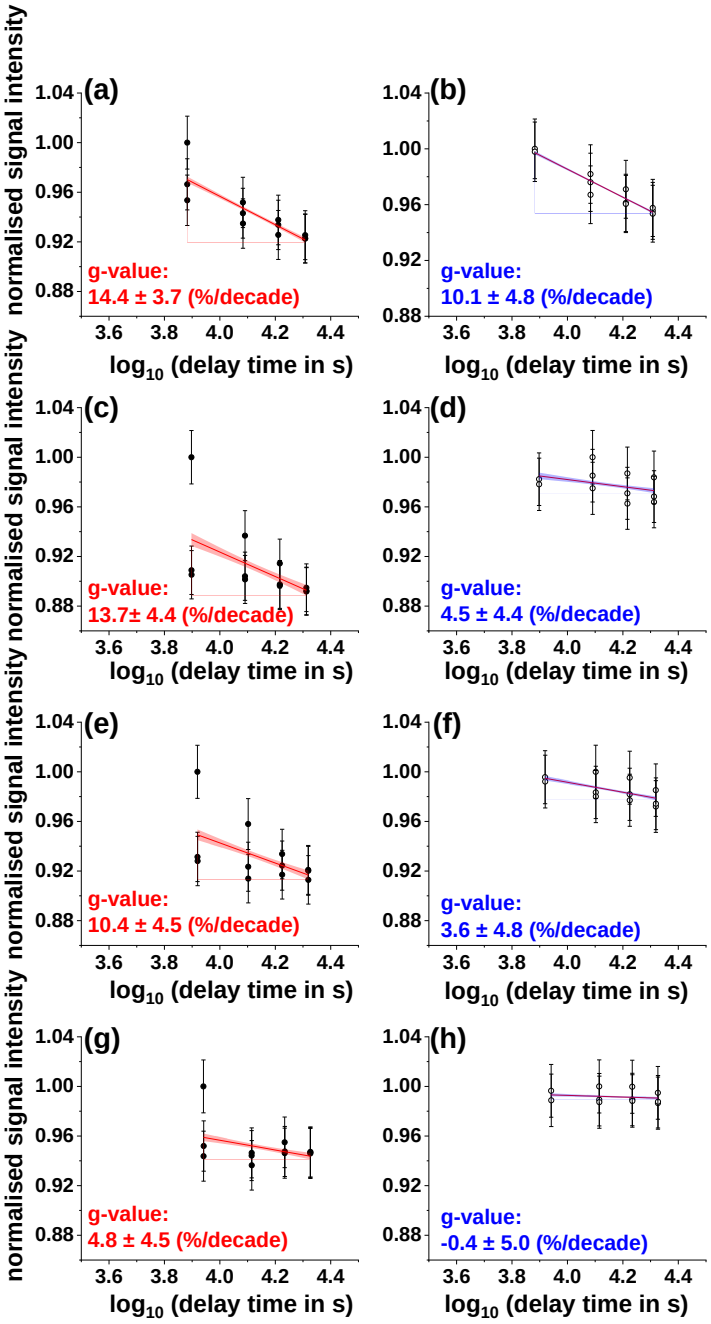

Figure S5. Anomalous fading measurements obtained for different IR stimulation temperatures with or without including the first prompt measurement, for a representative aliquot from sample GSSM. Normalized signal intensities are plotted as a function of time since irradiation for IR_{50} (a, b), pIR_{110} (c, d), pIR_{170} (e, f), and pIR_{225} (g, h) stimulations. Panels a, c, e and g show the linear regression and corresponding fading rates (g-values norm. 2 days) obtained including all signal readouts measured at different delay times, while panels b, d, f and h excluding the first prompt. Fading rates were calculated using the *analyse_FadingMeasurement* function in R package 'Luminescence' version 0.9.23 (Kreutzer et al., 2012).

Table S1 Luminescence dating results from the sand and matrix feldspar samples from the Roethig terrace (RTSL1, RTSL2 and RTSM). n/N= number of accepted over number of measured aliquots; OD = overdispersion; CAM = central age model (Galbraith et al., 1999). The reported g-values were estimated by excluding the first prompt measurement. Fading corrected ages produced from negligible g-value$_{2days}$ (<1.5%/decade) are also included in this table.

Sample ID	Sample type	Mineral	IRSL temperature	Dose rate (Gy/ka)	n/N	OD (%)	CAM D_e (Gy)	CAM age (ka)	g-value (%/decade)	Fading corrected age (ka)
RTSL-F1	Sand	Feldspar	IR_{50}	3.4 ± 0.2	20/20	7.94	33 ± 0.6	9.7 ± 0.4	4.6 ± 0.7	14.9 ± 1.6
			pIR_{110}		20/20	10	42.8 ± 1.0	12.7 ± 0.5	0.9 ± 0.8	13.6 ± 1.2
			pIR_{170}		20/20	23.1	50.5 ± 1.4	14.8 ± 0.6	0.2 ± 1.0	15.0 ± 1.4
			pIR_{225}		20/20	14.1	56 ± 1.8	16.4 ± 0.8	0.5 ± 1.1	17.1 ± 1.8
RTSL-F2	Sand	Feldspar	IR_{50}	3.2 ± 0.1	20/20	9.4	35.4 ± 0.8	10.9 ± 0.5	4.6 ± 0.7	16.8 ± 1.8
			pIR_{110}		20/20	6.2	46 ± 0.7	14.2 ± 0.5	0.9 ± 0.8	15.3 ± 1.2
			pIR_{170}		20/20	6.0	54.5 ± 0.8	16.8 ± 0.6	0.2 ± 1.0	17.1 ± 1.6
			pIR_{225}		20/20	12.4	60.6 ± 1.7	18.7 ± 0.8	0.5 ± 1.1	19.5 ± 2.1
RTSM-F	Matrix	Feldspar	IR_{50}	4.1 ± 0.2	20/20	20	34.3 ± 1.5	8.4 ± 0.5	4.3 ± 0.8	12.5 ± 1.5
			pIR_{110}		20/20	20.6	49.4 ± 2.3	12.0 ± 0.7	0.7 ± 0.8	12.7 ± 1.2
			pIR_{170}		20/20	20.5	59.2 ± 2.7	14.4 ± 0.8	0.4 ± 1.2	14.9 ± 1.8
			pIR_{225}		20/20	21.2	64.5 ± 3.2	15.7 ± 0.9	0.8 ± 1.1	16.8 ± 1.9

Table S2. Luminescence dating results from the sand and matrix feldspar samples from the Lingolsheim terrace (LHSL1, LHSL2, LHSL3 and LHSM). n/N= number of accepted over number of measured aliquots; OD = overdispersion; CAM = central age model (Galbraith et al., 1999). The reported g-values were estimated by excluding the first prompt measurement. Fading corrected ages produced from negligible g-value$_{2days}$ (<1.5%/decade) are also included in this table. *No fading correction was applied to samples and signals exhibiting negative fading rates.

Sample ID	Sample type	Mineral	IRSL temperature	Dose rate (Gy/ka)	n/N	OD (%)	CAM D_e	CAM age (ka)	g-value (%/decade)	Fading corrected age (ka)
LHSL-F1	Sand	Feldspar	IR_{50}	2.9 ± 0.1	20/20	9.4	64.9 ± 1.4	22.5 ± 1.0	4.5 ± 0.9	34.6 ± 4.7
			pIR_{110}		20/20	6.4	81.5 ± 1.3	28.3 ± 1.2	0.7 ± 1.2	30.0 ± 3.6
			pIR_{170}		20/20	6.7	95.5 ± 1.6	33.1 ± 1.4	-0.0 ± 1.3	33.1 ± 1.4*
			pIR_{225}		20/20	6.7	100.1 ± 1.7	34.7 ± 1.4	-1.5 ± 1.4	34.7 ± 1.4*
LHSL-F2	Sand	Feldspar	IR_{50}	2.9 ± 0.1	20/20	9.7	65.3 ± 1.5	22.6 ± 1.0	4.4 ± 1.0	34.4 ± 5.2
			pIR_{110}		20/20	7.3	81.8 ± 1.4	28.3 ± 1.2	1.3 ± 1.1	31.7 ± 3.7
			pIR_{170}		20/20	8.0	95.4 ± 1.8	33.0 ± 1.4	-0.0 ± 1.3	33.0 ± 1.4*
			pIR_{225}		20/20	6.4	101 ± 1.7	35.0 ± 1.4	-1.5 ± 1.2	35.0 ± 1.4*
LHSL-F3	Sand	Feldspar	IR_{50}	2.8 ± 0.1	20/20	11.9	53.6 ± 1.5	19.1 ± 0.9	5.0 ± 0.9	31.0 ± 4.5
			pIR_{110}		20/20	9.3	70 ± 1.5	25.0 ± 1.1	1.3 ± 1.1	28.0 ± 3.2
			pIR_{170}		20/20	9.7	81.9 ± 1.9	29.3 ± 1.3	1.6 ± 1.3	33.7 ± 4.7
			pIR_{225}		20/20	10.1	86.4 ± 2.1	30.9 ± 1.4	0.2 ± 1.2	31.4 ± 3.5
LHSM-F	Matrix	Feldspar	IR_{50}	3.4 ± 0.1	20/20	7.7	77.7 ± 1.4	23.1 ± 1.0	3.9 ± 1.1	33.3 ± 5.2
			pIR_{110}		19/20	9.2	97.2 ± 2.1	29.0 ± 1.2	0.6 ± 1.0	30.5 ± 3.0
			pIR_{170}		18/20	6.6	110.7 ± 1.9	33.0 ± 1.3	0.4 ± 1.3	34.1 ± 4.1
			pIR_{225}		18/20	11.1	116.9 ± 3.3	34.8 ± 1.6	-0.5 ± 1.2	34.8 ± 1.6*

Table S3. Table including the OD (%) values obtained from the dose recovery tests for the representative samples of three investigated terraces. A CAM of recovered dose (Gy) has been calculated from 3 quartz and feldspar aliquots from each terrace to produce the OD values. Quartz results are shown for dose recovery tests at 190°C preheat temperature, since the natural OSL D_e measurements were conducted on this specific temperature. Feldspar results are shown for dose recovery tests at all MET-pIRIR temperatures.

Sample ID	Preheat temperature (for Q) and IR stimulation temperature (for F) in °C	OD (%) obtained from dose recovery test
RTSL-Q1	190	$4.1e^{-11}$
RTSM-Q	190	$3.2e^{-10}$
LHSL-Q1	190	$4.1e^{-32}$
LHSM-Q	190	$9.5e^{-41}$
GHSL-Q1	190	$9.8e^{-32}$
GHSM-Q	190	$8.2e^{-46}$
RTSL-F1	50	$1.4e^{-67}$
	110	$1.2e^{-51}$
	170	$1.4e^{-69}$
	225	3.79
RTSM-F	50	$3.5e^{-80}$
	110	$9e^{-39}$
	170	$4.8e^{-11}$
	225	$2.4e^{-23}$
LHSL-F1	50	$1.7e^{-37}$
	110	$9.5e^{-7}$
	170	0.84
	225	1.97
LHSM-F	50	0.0005
	110	1.61
	170	$2.8e^{-64}$
	225	$1.7e^{-10}$
GHSL-F1	50	$1.9e^{-32}$
	110	$2.9e^{-11}$
	170	$4.1e^{-34}$
	225	1.31
GHSM-F	50	$3.3e^{-68}$
	110	$2.3e^{-36}$
	170	$9.3e^{-93}$
	225	$3.2e^{-56}$

Table S4. Summarization of D_e values both using a central age model (CAM) and an average dose model (ADM) for the matrix samples from the three terraces. Note that, the comparison has been shown for the matrix samples particularly those produced higher OD values (≥ 20%) for their CAM D_e calculation.

Sample ID	IRSL temperature	OD (%)	CAM D_e (Gy)	CAM age (Ka)	ADM D_e (Gy)	ADM age (ka)	Δage (ADM-CAM) (Ka)	% of difference
RTSM-Q	--	22.9	36.1 ± 1.8	10.8 ± 0.7	37.0 ± 1.6	10.9 ± 0.6	0.1	0.9
RTSM-F	IR_{50}	20	34.3 ± 1.5	8.4 ± 0.5	35.0 ± 1.4	8.5 ± 0.4	0.1	1.1
	pIR_{110}	20.6	49.4 ± 2.3	12.0 ± 0.7	50.4 ± 2.3	12.2 ± 0.7	0.2	1.6
	pIR_{170}	20.5	59.2 ± 2.7	14.4 ± 0.8	60.4 ± 2.8	14.7 ± 0.8	0.3	2.0
	pIR_{225}	21.2	64.5 ± 3.2	15.7 ± 0.9	66.0 ± 3.8	16.0 ± 1.1	0.3	1.9
LHSM-Q	--	21.7	85.6 ± 4.8	32.5 ± 2.1	86.6 ± 4.9	32.7 ± 2.2	0.2	0.6
GHSM-F	pIR_{110}	20.6	932 ± 48	343 ± 22	951 ± 47	350 ± 21	7.0	2.0
	pIR_{170}	35.9	1283 ± 163	472 ± 21	1362 ± 111	501 ± 44	29.0	6.1

Table S5 The table summarizes the g-values$_{2days}$ obtained on sample RTSL-F1 using two different maximum delay time (i.e. 3 h and 24 h) for its fading measurement. Each g-value$_{2days}$ was obtained using R studio 'Luminescence' package 0.9.23 by combing the fading data (consisting the signal, signal associated error and time in second) from 3 separate RTSL-F1 aliquots, previously used for dose recovery test. Two different IR50 fading corrected ages are produced using the non-normalized g-value. This quantitative comparison evaluates how the use of different delay time impacted the fading correction while estimating the IR50 fading-corrected age of the sample RTSL-F1.

IR stimulation temperature	g-value$_{2days}$ (with max. delay time 3 h) (%/decade)	IR$_{50}$ fading corrected age based on g-value measured with max. delay time 3 h (ka)	g-value$_{2days}$ (with max. delay time 24 h) (%/decade)	IR$_{50}$ fading corrected age based on g-value measured with max. delay time 24 h (ka)
IR$_{50}$	4.6 ± 0.7	14.9 ± 1.6	3.9 ± 0.5	13.9 ± 1.0
pIR$_{110}$	0.9 ± 0.8		0.9 ± 0.5	
pIR$_{170}$	0.2 ± 1.0		0.6 ± 0.6	
pIR$_{225}$	0.5 ± 1.1		-0.9 ± 0.7	

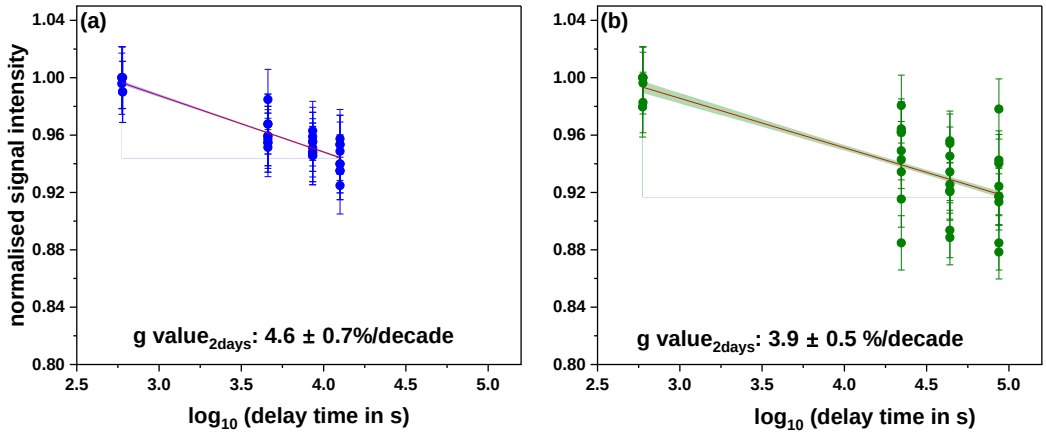

Figure S6. Anomalous fading measurements obtained for sample RTSL-F1 using different maximum delay times. Normalised signal intensities are plotted as a function of time since irradiation for IR$_{50}$ stimulation. Panel (a) and (b) show the linear regression and corresponding fading rates (g-value$_{2days}$) obtained using a maximum delay time of 3 h and 24 h respectively after excluding the first prompt measurement from fading data. Fading measurements from three aliquots were combined and represented in this figure. The slope of the fading regression line deviates a little between panel (a) and (b) and the resulted g-values are overlapping within 1σ uncertainty while measured using different maximum delay times.